Zhejiang Provincial Engineering Technology Research Center of Marine Biomedical Products[1], School of Food and Pharmacy, Zhejiang Ocean University; Zhoushan Institute for Food and Drug Control[2], Zhoushan, China

Astaxanthin attenuated hyperuricemia and kidney inflammation by inhibiting uric acid synthesis and the NF-κB/NLRP3 signaling pathways in potassium oxonate and hypoxanthine-induced hyperuricemia mice

Jiangchao Zhuang[1,#], Xie Zhou[1,#], Ting Liu[2], Shuai Zhang[1], Falei Yuan[1], Leifang Zhang[1], Zuisu Yang[1], Yan Chen[1,*]

Received July 14, 2021, accepted august 21, 2021

**Corresponding author: Yan Chen, Zhejiang Provincial Engineering Technology Research Center of Marine Biomedical Products, School of Food and Pharmacy, Zhejiang Ocean University, Zhoushan 316022, China*
cyancy@zjou.edu.cn
[#]These authors contributed equally to this work.

Pharmazie 76: 551-558 (2021) *doi: 10.1691/ph.2021.1731*

Inflammation is an important pathological feature of hyperuricemia, which in turn aggravates hyperuricemia. Astaxanthin is a carotenoid with strong antioxidant capacity and possesses many biological activities. This study was aimed to evaluate the effect of astaxanthin (ASX) on hyperuricemia and kidney inflammation in potassium oxonate (PO) and hypoxanthine (HX)-induced hyperuricemic mice. Male ICR mice were administered intragastrically with PO and HX (250 mg/kg, respectively) for 14 days. ASX was given by gavage one hour after PO and HX administration. ASX treatment significantly reversed PO and HX-induced hyperuricemia and kidney inflammation in mice as evidenced by decreased serum levels of uric acid (UA), creatinine (Cr), blood urea nitrogen (BUN), and inflammatory factors (IL-1β, IL-6, and TNF-α) and increased activities of antioxidant enzymes (CAT, SOD and GSH-Px). Furthermore, ASX administration effectively inhibited the activities of key enzymes related to UA synthesis (xanthine oxidase (XOD) and adenosine deaminase (ADA)) and modulated the protein expressions of NF-κB p65, p-NF-κB p65, IκBα, p-IκBα, NLRP3, ASC, Caspase-1, and cleaved-Caspase-1 involved in inflammation pathways. Our results suggested that ASX improved hyperuricemia and kidney inflammation induced by PO and HX, probably by reducing UA synthesis and suppressing the NF-κB and NLRP3 pathways simultaneously.

1. Introduction

Hyperuricemia, characterized as serum uric acid (UA) level exceeds 7 mg/dL, is a metabolic disease caused by abnormal purine metabolism or UA excretion in humans (Kim et al. 2019). Nowadays, the prevalence of hyperuricemia increases rapidly due to transformation of diet, mainly the ingestion of a large amount of purines, which ultimately leads to the overproduction of UA (Liu et al. 2014). Excess UA in blood stimulates the mesangial cells to generate a large amount of reactive oxygen species (ROS), which cause oxidative damage, activation of NOD-like receptor family pyrin domain containing 3 (NLRP3) inflammasome, and release of IL-1β in kidney (Cui et al. 2020; Dalbeth et al. 2019). Meanwhile, a high level of serum UA promotes the release of pro-inflammatory cytokines *via* the Nuclear Factor Kappa-B (NF-κB) signaling pathway (Chen et al. 2017; Linker et al. 2012; Zhang et al. 2018). The triggered inflammatory and oxidative stress responses by UA consequently lead to kidney inflammation, which in turn causes the reduction of UA excretion in the kidney (Wu et al. 2016; Yip et al. 2020; Zhou et al. 2012). Hence, controlling serum UA levels and reducing kidney inflammation are considered as two key strategies in terms of hyperuricemia treatment (Yip et al. 2020).

Currently, based on the mechanism of action, the clinical drugs for hyperuricemia treatment can be mainly divided into three categories: drugs that block UA synthesis (allopurinol), drugs that facilitate UA excretion (benzbromarone), and drugs that reduce kidney inflammation (cortin). However, the use of these drugs shows many adverse effects, such as severe cutaneous adverse reactions, liver toxicity and gastrointestinal disorders (Hung et al. 2005; Xiao et al. 2020). Thus, it has attracted increasing attention to find safer agents that contribute to the alleviation of hyperuricemia and kidney inflammation. In recent years, functional foods and nutraceuticals from natural creatures have been considered as potential alternatives for improving hyperuricemia and kidney inflammation (Chau et al. 2019; He et al. 2019; Jiang et al. 2020; Le et al. 2020). Carotenoids, such as β-carotene and fucoxanthin, have been demonstrated to exhibit satisfactory effect of lowering UA (Chau et al. 2019; Choi et al. 2012; Le et al. 2020). Our previous study has demonstrated the preventive effects of astaxanthin (ASX) on high-fructose-induced hyperuricemia in rat models through decreasing UA synthesis and increasing UA excretion. However, the effectiveness and possible mechanism of ASX in the treatment of kidney inflammation caused by hyperuricemia has not been studied, although previous studies have demonstrated the great potential of ASX on alleviating kidney damage caused by a variety of reasons, including severe burning, cisplatin treatment, diabetes, and ochratoxin A (Akca et al. 2018; Chen et al. 2020; Guo et al. 2021; Li et al. 2020). To be noted, NLRP3 inflammasome contributes to a variety of kidney diseases, activated NLRP3 signaling pathway regulate the expressions of inflammatory factors along with the nuclear translocation of NF-κB (Chen et al. 2017; Chen et al. 2019). Combined with the fact that the NLRP3 and NF-κB signaling pathways are served as the main pathways involved in kidney inflammation (Cabau et al. 2020; Chen et al. 2019; Cui et al. 2020), we supposed that the renal inflammation induced by hyperuricemia could be improved by ASX *via* regulating the NLRP3 and NF-κB signaling pathways.

In this study, a mouse model of hyperuricemia had been built by potassium oxonate (PO) and hypoxanthine (HX). To investigate the effect of ASX on hyperuricemia and kidney inflammation in

hyperuricemic mice, kidney index, serum and kidney biochemical indicators, and kidney morphology were detected. To further explore its underlying mechanism, the enzyme activities of liver xanthine oxidase (XOD) and adenosine deaminase (ADA) and the expression of key proteins on NF-κB and NLRP3 signaling pathways in kidney tissues homogenate were measured. Our study aims to discuss the effectiveness and potential mechanism of ASX in the treatment of hyperuricemia and kidney inflammation from the perspective of UA synthesis and the NF-κB and NLRP3 inflammatory pathways.

2. Investigation and results

2.1. Effect of ASX on body weight, kidney index, serum UA, Cr and BUN

As shown in Fig. 1, compared to the control group, the model group demonstrated significantly increased kidney index and serum levels of UA, creatinine (Cr) and blood urea nitrogen (BUN) after 14 days' treatment of PO and HX, in addition to a relatively decreased body weight ($P < 0.05$). However, the situation was reversed by oral administration with allopurinol (ALL) or different doses of ASX. The body weight, kidney index and serum levels of UA, Cr and BUN in mice treated with ALL recovered to a level similar to those of normal mice ($P > 0.05$). Similar results were observed in those ASX treatment groups. Specifically, the mice final body weight in the ASX groups were found to be significantly increased, and the serum UA and kidney functional indicators showed a significant decrease in a dose-dependent manner. Notably, the serum UA level in mice treated with ASX high dose returned to a level similar to that of the ALL group, which is close to normal level (Fig. 1c).

2.2. Effect of ASX on XOD and ADA activities in liver

The effect of ASX on UA synthesis was explored by accessing the activities of XOD and ADA in the liver. The activities of XOD and ADA were remarkably increased in the liver tissues

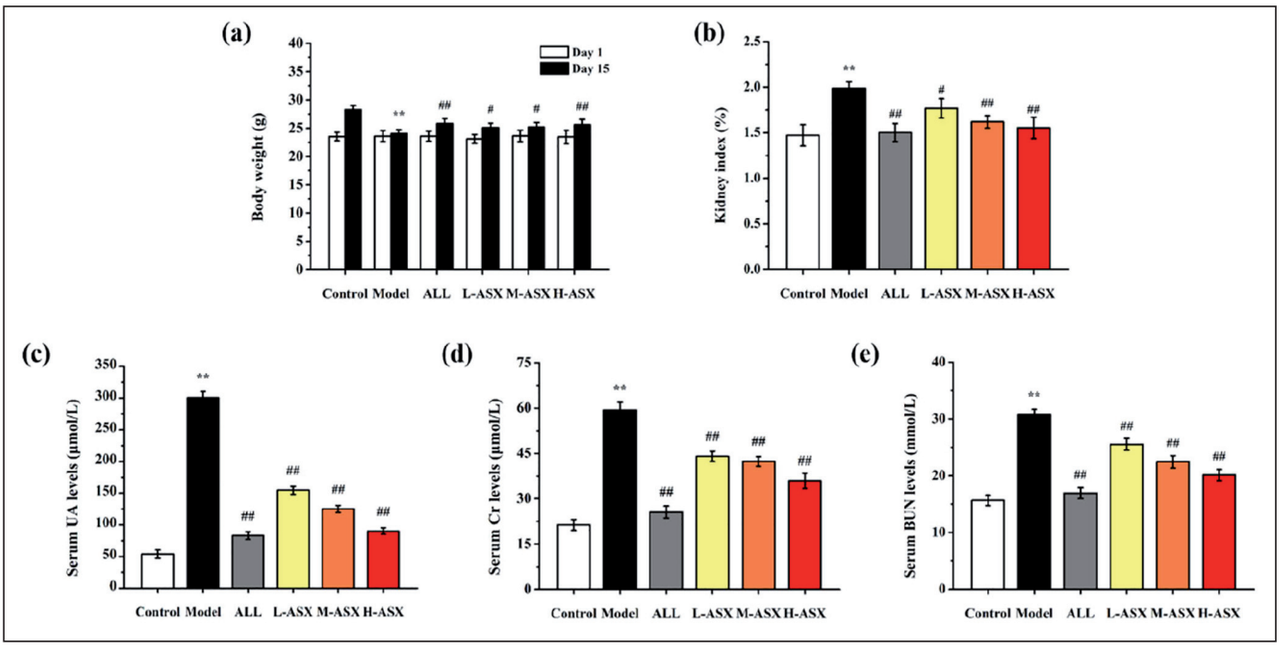

Fig. 1: Effect of ASX on body weight (a), kidney index (b), serum UA (c), Cr (d) and BUN (e) in hyperuricemic mice. Values are presented as the mean±SEM (n = 8). * $P < 0.05$, ** $P < 0.01$ *vs.* control group; # $P < 0.05$, ## $P < 0.01$ *vs.* model group. ALL: allopurinol; L-ASX, M-ASX, and H-ASX: astaxanthin at the doses of 25, 50, and 100 mg/kg, respectively.

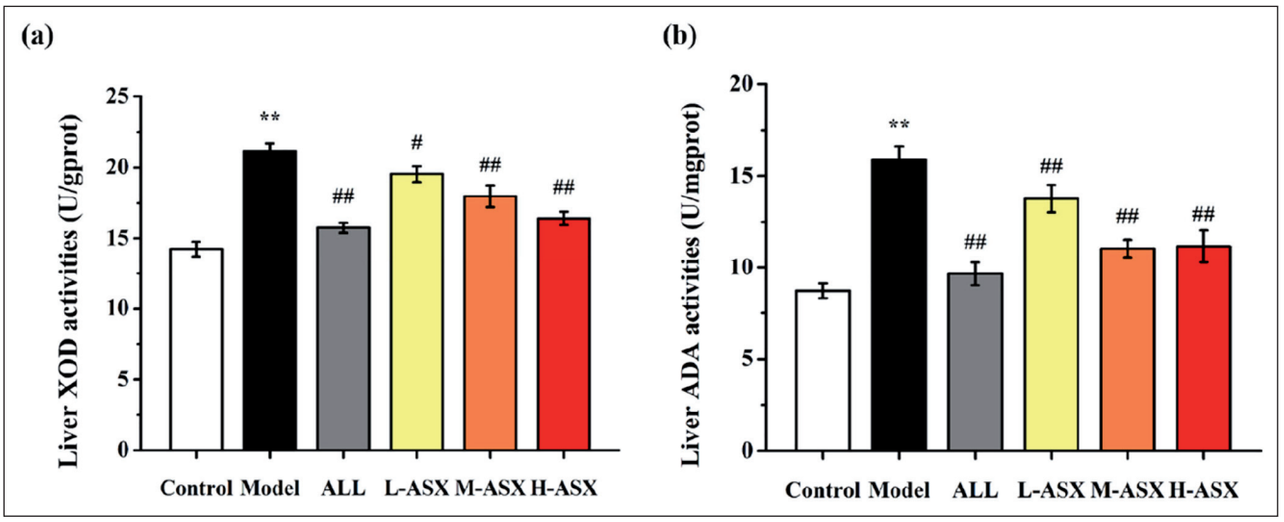

Fig. 2: Effect of ASX on liver XOD (a) and ADA (b) activities. Values are presented as the mean±SEM (n = 8). * $P < 0.05$, ** $P < 0.01$ *vs.* control group; # $P < 0.05$, ## $P < 0.01$ *vs.* Model group. ALL: allopurinol; L-ASX, M-ASX, and H-ASX: astaxanthin at the doses of 25, 50, and 100 mg/kg, respectively.

of PO and HX-induced hyperuricemic mice compared to normal mice ($P < 0.01$) (Fig. 2). Interestingly, after treated with different doses of ASX, the activities of XOD and ADA were significantly suppressed compared to the Model group ($P < 0.05$) (Fig. 2). Among the ASX treatment groups, ASX high dose exhibited the strongest inhibition effects on the enzymatic activities of XOD and ADA, and the activities of both enzymes in the H-ASX group were close to that in the ALL group. These results are consistent with our previous findings in fructose-induced hyperuricemic rat models (Le et al. 2020).

2.3. Effect of ASX on the histopathology of the kidney

The inflammatory cell infiltration and tissue damage are considered as pathological features of hyperuricemia (Chen et al. 2019). As shown in Fig. 3, mice in control group displayed normal glomerular and tubular epithelial structures in kidney, the brush borders of the renal tubules were neatly and regularly arranged. However, mice treated with PO and HX showed obvious tubular lesions including inconspicuous boundaries between adjacent proximal tubule cells, tubular expansion, and aggregation of the inflammatory cells around the renal blood vessels. Post-treatment with ALL and ASX attenuated renal tubular injury and inflammatory cell infiltration in variable degrees.

2.4. Effect of ASX on MDA level and antioxidant enzymes activities in kidney

The main antioxidant enzymes, including superoxide dismutase (SOD), catalase (CAT) and glutathione peroxidase (GSH-Px), are crucial indicators for evaluating the capacity of the cellular antioxidant defense system, which are related to the production of lipid peroxidation product malondialdehyde (MDA) (Chen et al. 2019; Zheng et al. 2019). As depicted in the Table, compared to the normal mice, the kidney MDA level in PO and HX-challenged mice were significantly increased, while the activities of SOD, GSH-Px, and CAT in kidney were obviously decreased. In contrast, treatment with ASX for 14 days markedly reduced kidney MDA contents and enhanced the activities of SOD, CAT, and GSH-Px in a dose-dependent manner ($P < 0.01$). The kidney MDA content and the activities of kidney SOD, GSH-Px, and CAT in H-ASX group were similar to that of the ALL group.

2.5. Effect of ASX on pro-inflammatory cytokines in serum and kidney

To assess the effect of ASX on kidney inflammation, the levels of inflammatory cytokines (interleukin-1β (IL-1β), interleukin-6 (IL-6), and tumor necrosis factor-α (TNF-α)) in both serum and kidney tissue homogenate were measured. After PO and HX treat-

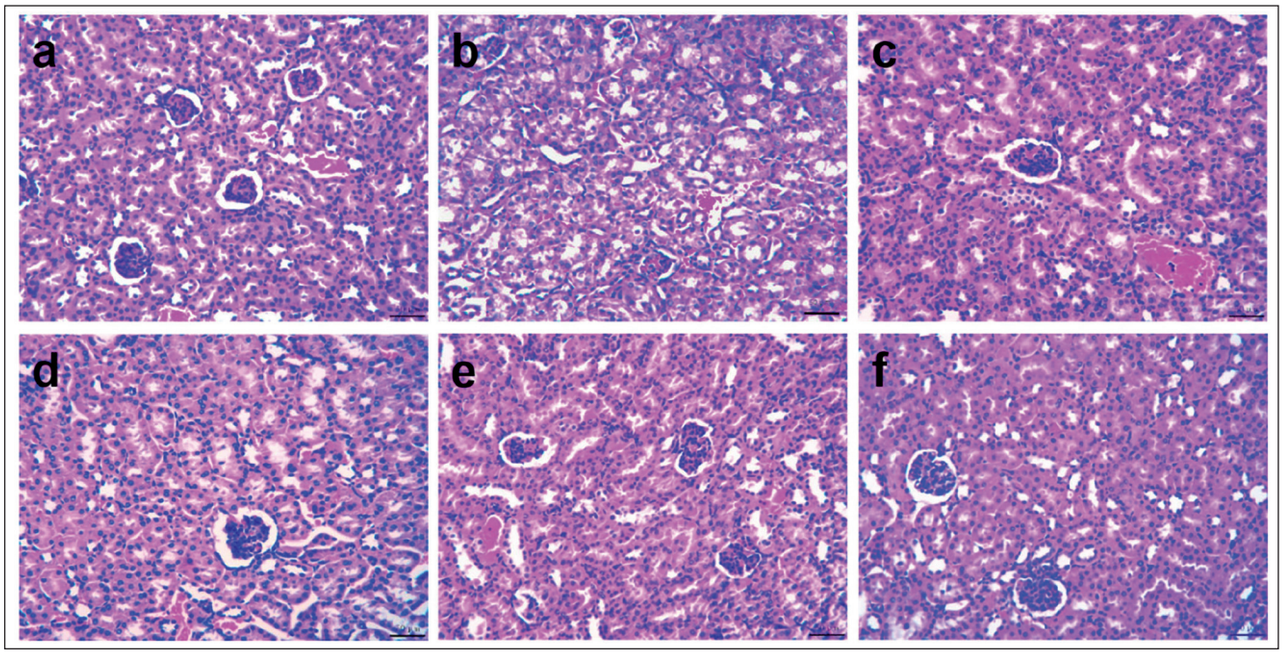

Fig. 3: Effect of ASX on histological changes. H&E staining images of kidney sections of the Control group (a), the Model group (b), the ALL group (c), the L-ASX group (d), the M-ASX group (e) and the H-ASX group (f) at original magnification 200×. ALL: allopurinol; L-ASX, M-ASX, and H-ASX: astaxanthin at the doses of 25, 50, and 100 mg/kg, respectively.

Table: Effect of ASX on MDA level and antioxidant enzymes activities in kidney

Group	SOD (U/mg prot)	GSH-Px (U/mg prot)	CAT (U/mg prot)	MDA (nmol/mg prot)
Control	101.33 ± 5.16	94.21 ± 5.83	38.18 ± 1.04	2.55 ± 0.12
Model	67.19 ± 4.64**	62.52 ± 3.98**	25.78 ± 1.43**	4.69 ± 0.27**
ALL	98.37 ± 6.27##	91.32 ± 3.38##	37.15 ± 1.06##	2.63 ± 0.21##
L-ASX	80.16 ± 6.51##	78.63 ± 3.34##	31.34 ± 1.02##	3.99 ± 0.31#
M-ASX	90.51 ± 3.91##	84.21 ± 6.23##	33.23 ± 1.31##	3.25 ± 0.42##
H-ASX	97.47 ± 5.15##	90.06 ± 5.28##	35.95 ± 1.18##	2.75 ± 0.28##

Values are presented as the mean±SEM (n = 8). * $P < 0.05$, ** $P < 0.01$ vs. control group; # $P < 0.05$, ## $P < 0.01$ *vs.* model group. ALL: allopurinol; L-ASX, M-ASX, and H-ASX: astaxanthin at the doses of 25, 50, and 100 mg/kg, respectively.

ment, the levels of IL-1β, IL-6, and TNF-α in serum and kidney tissues were markedly increased compared to normal mice ($P < 0.01$) (Fig. 4). ASX treatment significantly decreased IL-1β, IL-6, and TNF-α levels in both serum and kidney of the PO and HX-challenged mice ($P < 0.01$) (Fig. 4). To be noted, the levels of inflammatory cytokines in the H-ASX group and ALL group were close.

2.6. Effect of ASX on the NF-κB signaling pathway in hyperuricemic mice

To interpret the anti-inflammatory mechanism of ASX against kidney inflammation in PO and HX-induced hyperuricemic mice, the key proteins of NF-κB pathway was studied. The expressions of key proteins involved in NF-κB signaling (p-NF-κB p65, NF-κB

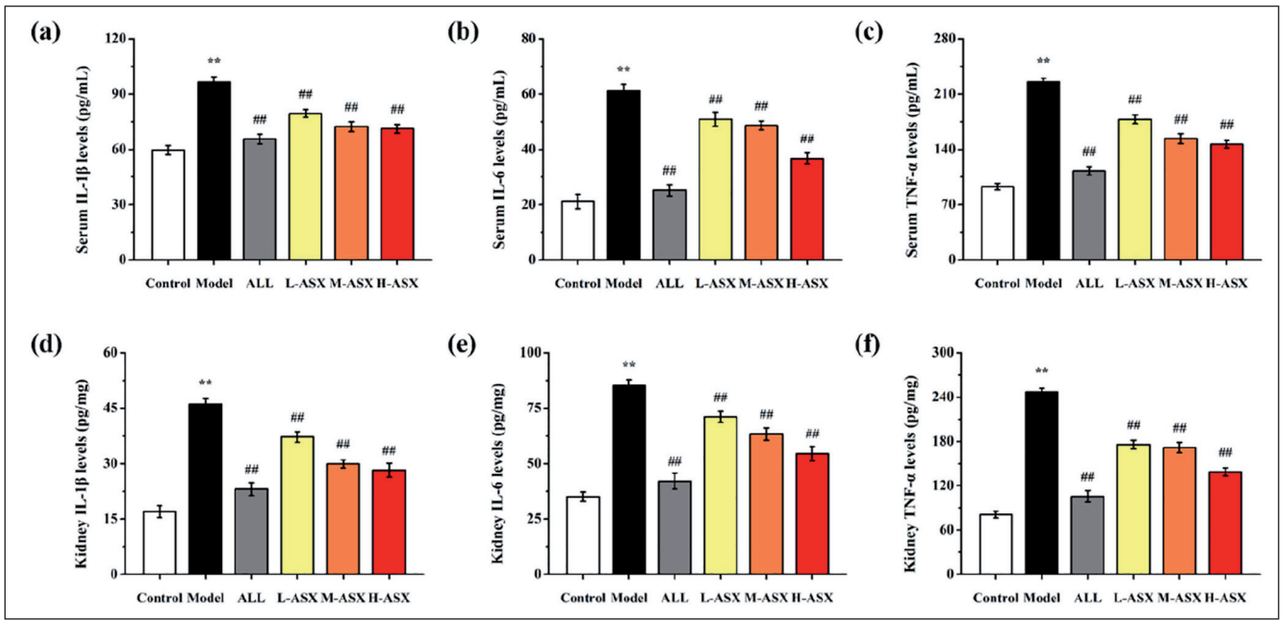

Fig. 4: Effect of ASX on pro-inflammatory cytokines levels in both serum and kidney. The levels of IL-1β (a), IL-6 (b), and TNF-α (c) in serum and the levels of IL-1β (d), IL-6 (e), and TNF-α (f) in kidney were determined by ELISA. Values are presented as the mean±SEM (n = 8). * $P < 0.05$, ** $P < 0.01$ *vs.* control group; # $P < 0.05$, ## $P < 0.01$ *vs.* model group. ALL: allopurinol; L-ASX, M-ASX, and H-ASX: astaxanthin at the doses of 25, 50, and 100 mg/kg, respectively.

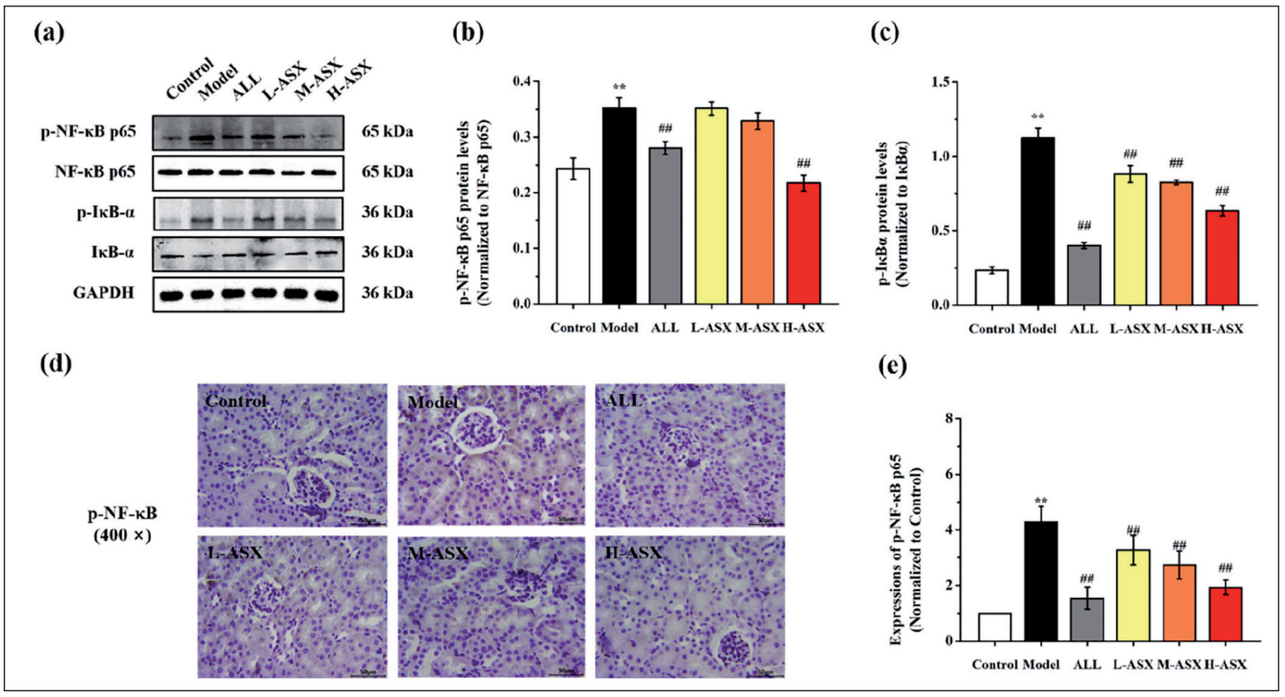

Fig. 5: Effect of ASX on protein expressions of the NF-κB signaling pathway in kidney. (a) Western blot analysis of p-NF-κB p65, NF-κB p65, p-IκBα, and IκBα. (b) The relative protein expression of p-NF-κB p65, the content of target protein was normalized to NF-κB p65. (c) The relative protein expression of p-IκBα, the content of target protein was normalized to IκBα. (d) Immunohistochemical examination of p-NF-κB p65 in kidney sections. Magnification, 400×. (e) Semi-quantitative analysis for p-NF-κB p65 immunohistochemical staining. * $P < 0.05$, ** $P < 0.01$ *vs.* control group; # $P < 0.05$, ## $P < 0.01$ *vs.* model group. ALL: allopurinol; L-ASX, M-ASX, and H-ASX: astaxanthin at the doses of 25, 50, and 100 mg/kg, respectively.

p65, p-IκBα, and IκBα) in kidney were analyzed by western blotting. As illustrated in Fig. 5a-5c, the expressions of p-NF-κB p65 and p-IκBα in the model group were significantly higher than those in the control group ($P < 0.01$). To be noted, the hyperuricemic mice treated with different doses of ASX demonstrated significantly down-regulated expression levels of p-NF-κB p65 and p-IκBα in a dose-dependent manner compared to the model group ($P < 0.01$). The results of immunohistochemical detection of p-NF-κB p65 protein expressions in kidney were shown in Fig. 5d-5e. The protein expression of p-NF-κB p65 increased significantly in the kidney of PO and HX-induced hyperuricemic mice in comparison to the control group. ASX treatment significantly suppressed the upregulated expression of p-NF-κB p65 in hyperuricemic mice ($P < 0.01$) as expected. The immunohistochemistry results were consistent with the results of western blotting, indicating that ASX could prevent kidney inflammation through inhibiting the activation of the NF-κB signaling pathway.

2.7. Effect of ASX on the NLRP3 inflammatory pathway in hyperuricemic mice

To further investigate the renal protective mechanism of ASX in hyperuricemic mice, the expressions of proteins related to the NLRP3 inflammatory pathway were analyzed. As a result, the expressions of NLRP3 inflammasome associated proteins (NLRP3, ASC, Caspase-1, and cleaved-Caspase-1) in PO and HX-induced hyperuricemic mice were significantly upregulated compared to the Control group ($P < 0.01$) (Fig. 6a-6e). Following the treatment with ASX in different dosages, the expressions of these proteins were remarkably down-regulated as compared to the model group ($P < 0.05$) (Fig. 6a-6e). In addition, the results of semi-quantitative analysis for NLRP3 immunohistochemical staining were in accordance with the results of western blotting, and NLRP3 were mainly expressed in the renal tubules (Fig. 6f-6g). These results suggested that ASX treatment could improve kidney inflammation through inhibiting the activation of the NLRP3 signaling pathway.

3. Discussion

Nowadays, the prevalence of hyperuricemia elevated rapidly throughout the world and has become a global public health problem. High purine diet is the main cause of hyperuricemia due to the excessive production of UA in the body as a result of purine metabolism (Lin et al. 2000). Increased supply of UA precursors (xanthine, HX, *etc.*) could effectively enhance the metabolic flux of UA synthesis and eventually lead to excessive UA accumulation (Chen et al. 2019). UA cannot be degraded into allantoin that has better solubility due to the lack of uricase in humans. Coupled with

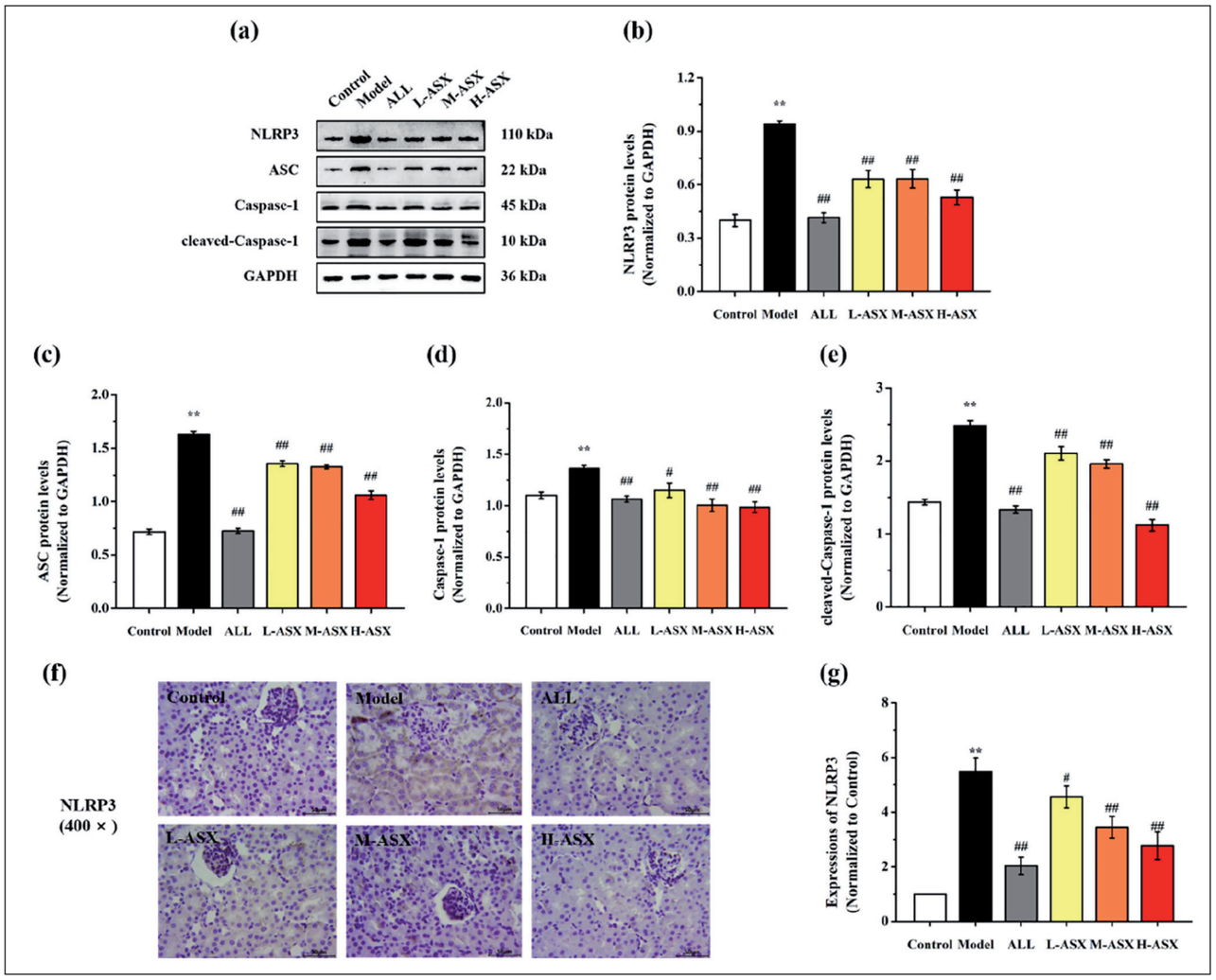

Fig. 6: Effect of ASX on the NLRP3 inflammasome in the kidney of hyperuricemia mice. (a) Western blot analysis of NLRP3, ASC, Caspase-1, and cleaved-Caspase-1. (b) The relative expression level of NLRP3. (c) The relative expression of ASC. (d) The relative expression of Caspase-1. (e) The relative expression of cleaved-Caspase-1. The content of target protein was normalized to GAPDH. (f) Immunohistochemical examination of NLRP3 in kidney sections. Magnification, 400×. (g) Semi-quantitative analysis for NLRP3 immunohistochemical staining. * $P < 0.05$, ** $P < 0.01$ *vs.* control group; # $P < 0.05$, ## $P < 0.01$ *vs.* model group. ALL: allopurinol; L-ASX, M-ASX, and H-ASX: astaxanthin at the doses of 25, 50, and 100 mg/kg, respectively.

the limited ability of UA excretion in kidney and intestine, humans are prone to suffer from hyperuricemia (Liu et al. 2017). Remarkably, due to the initial symptoms are often non-specific and painless, excessive accumulation of UA usually lasts for a long time and develops into severe kidney inflammation (Yip et al. 2020). To make matters worse, nephritis reduces the excretion of UA in the kidneys (Oh et al. 2019). Therefore, lowering serum UA level while controlling inflammation is a better strategy in the treatment of hyperuricemia. Since PO is the inhibitor of uricase and HX is purine supplement, in this study, PO and HX administration were used to simulate the process of excess UA formation in human to establish hyperuricemic mice model (Meng et al. 2017; Qian et al. 2019). After 14 days treatment of PO and HX, the mice body weight, kidney index, serum and kidney biochemical indicators, kidney tissue architecture, and other results exhibited unfavorable changes. Related literatures using PO and HX for hyperuricemia modeling also reported similar results (Chau et al. 2019; Chen et al. 2019). These results suggest that the hyperuricemic mice model with kidney inflammation was established successfully by oral administration of PO and HX. To be noted, those unfavorable changes mentioned above have been reversed by ASX. Specifically, mice treated with different doses of ASX showed an ameliorative effect in hyperuricemia and kidney inflammation which reflected in the restoration of body weight, kidney index, serum and kidney biomarkers, and kidney histomorphology. These results indicate that ASX exerted a remarkable effect in the improvement of hyperuricemia and kidney inflammation.

Clinically, serum UA level is the key indicator for evaluating disease activity of hyperuricemia. ASX administration ameliorated PO and HX-induced hyperuricemia by decreasing serum UA level, indicating that ASX could be serve as a potential drug substitute for the treatment of hyperuricemia. Abnormal UA synthesis in liver is a major cause of excess UA accumulation *in vivo*. In the purine nucleotide metabolic pathway, ADA and XOD are key enzymes involved in conversion of purine to UA. Adenosines are deaminated to inosines by ADA, which are then metabolized into HX and xanthine, and finally HX and xanthine are further converted to UA by XOD (Wei et al. 2018). In this study, ASX treatment significantly decreased the activities of XOD and ADA in PO and HX-induced hyperuricemic mice, which is in accordance with our previous findings in fructose-induced hyperuricemic rats (Le et al. 2020). In our previous study, ASX has been proved to reduce UA synthesis not only by inhibiting the activities of XOD and ADA, but also by suppressing the mRNA expressions of XOD and ADA (Le et al. 2020). These results suggest that the effect of ASX on lowering serum UA concentration is largely due to the down-regulated UA synthesis in PO and HX-induced hyperuricemia mice, thereby improving hyperuricemia.

Similarly, serum Cr and BUN are commonly regarded as indicators of kidney function (Tang et al. 2016). Increased levels of Cr and BUN indicate abnormal kidney function and a reduced excretion capacity of kidney (Yuan et al. 2018). The present study shows that treatment with ASX effectively decreased serum Cr and BUN levels in hyperuricemic mice. Furthermore, the histopathological results revealed that ASX diet has a protective effect against hyperuricemia-induced kidney inflammation which reflected in the restoration of kidney architecture.

The inflammatory response is a characteristic pathologic feature of hyperuricemia (Zhou et al. 2012). It is reported that excess UA promotes the secretion of inflammatory factors (IL-6, IL-1β, and TNF-α) in kidney, and further result in nephritis (Chen et al. 2019; Zhou et al. 2012). IL-1β as a strong pro-inflammatory factor can induce a variety of pro-inflammatory mediators, which recruit immune cells to the sites of inflammation and initiate a local inflammatory response (Anders et al. 2018; Pelegrin et al. 2009). TNF-α and IL-6 are also involved in inflammation and promote the proliferation of glomerular mesangial matrix (Domingueti et al. 2016). In this study, ASX treatment was found to be significantly decreased the levels of IL-6, IL-1β, and TNF-α in PO and HX-induced hyperuricemic mice. It has been reported that the reduction of inflammatory factors contribute to inflammation improvement and better kidney protection (Das et al. 2019). Therefore, our results suggest that ASX could decrease the level of pro-inflammatory factors and reduce inflammatory response in PO and HX-induced hyperuricemic mice, and thus contributing to the improvement of kidney inflammation.

The incidence of hyperuricemia is associated with high levels of oxidative stress mediators, and kidney is one of the main organs affected by hyperuricemia-induced oxidative stress (Zhang et al. 2019). When kidney cells are suffered from oxidative stress, the synthesis and release of inflammatory factors will be further enhanced, and consequently exacerbating inflammation (Chih et al. 2017). MDA is an important metabolic product of the oxidative stress response, and its accumulation causes cell damage and apoptosis (Zheng et al. 2019). Antioxidant enzymes (CAT, SOD, and GSH-Px) have been reported to contribute to scavenging ROS and lowering MDA content, thereby defending against oxidative damage and protecting both the structure and function of kidney cells (Li et al. 2020). Restoring the activities of CAT, SOD, and GSH-Px can reduce the production of ROS, and thus reducing oxidative stress damage and kidney inflammation in PO-induced hyperuricemic mice (Chen et al. 2019). In this study, the MDA contents and the activities of antioxidant enzymes in the ASX groups were similar to those in normal group, indicating that ASX could reduce kidney oxidative damage through improving the antioxidant capacity. The improvement of oxidative damage could further contribute to the reduced secretion of inflammatory factors and thus improving kidney inflammation.

The NF-κB pathway is important in regulating inflammation response. Excess UA can stimulate the activation of NF-κB signaling pathway (Kim et al. 2017). Besides, overproduced ROS can stimulate the NF-κB signaling as well and consequently promote the secretion of inflammatory cytokines, such as TNF-α, IL-8, and IL-6 (Molteni et al. 2016). The degradation of IκB causes the separation of NF-κB from IκB and then NF-κB can be translocated into the nucleus where it can regulate the expressions of various inflammatory mediators (Li et al. 2019). Jiang et al. documented that the downregulated NF-κB p65 and IκBα phosphorylation can reduce the release of nuclear factors and inflammatory cytokines, thereby ameliorating tissue inflammatory damage (Jiang et al. 2020). Hence, the NF-κB signaling pathway was chosen as a therapeutic target to prevent kidney inflammatory in PO and HX-induced hyperuricemia mice in this study. Our results of western blotting and immunohistochemistry suggest that ASX can inhibit the NF-κB pathway, as indicated by the decreased expressions of p-NF-κB p65 and p-IκBα in the kidney of PO and HX-induced hyperuricemic mice, and thus contributing to the amelioration of kidney inflammation.

The canonical NLRP3 pathway is downstream of the NF-κB pathway (Sutterwala et al. 2014). NLRP3 inflammasome is the best characterized inflammasome consisting of NLRP3, ASC, and caspase-1 (Zhao et al. 2017). The activation of NLRP3 inflammasome leads to the activation of Caspase-1 in addition to the upregulation of many inflammatory mediators (Hornung et al. 2008). Inhibiting the activation of NLRP3 inflammasome has been reported to reduce inflammatory mediators, and thus alleviating kidney inflammation (Chen et al. 2019). After the treatment of ASX, the expressions of the NLRP3, ASC, Caspase-1, and cleaved-Caspase-1 in the NLRP3 signaling pathway were significantly downregulated, suggesting that ASX could suppress the activation of the NLRP3 pathway. Overall, our results manifest that the anti-inflammatory effect of ASX against hyperuricemia-induced kidney inflammation is achieved by suppressing both the NF-κB and NLRP3 signaling pathways.

In conclusion, our experiments confirmed that ASX has the potential to improve hyperuricemia and accompanied kidney inflammation (Fig. 7), which reflected in the restoration of serum UA level, kidney-related biomarkers, and kidney morphology. The ameliorating effects of ASX in lowering serum UA concentration and improving renal inflammation may be achieved by inhibiting the activities of XOD and ADA and modulating the NF-κB and NLRP3 signaling pathways, respectively. Our results suggest that ASX could serve as a fabulous drug substitute due to its dual effects on hyperuricemia and kidney inflammation.

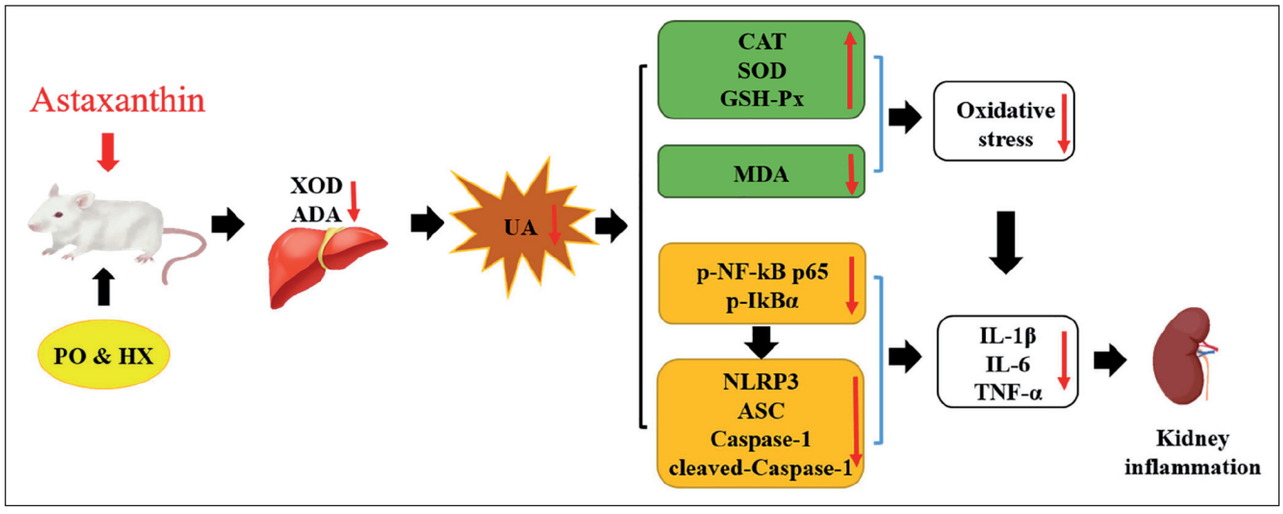

Fig. 7: ASX ameliorates PO and HX-induced hyperuricemia and kidney inflammation in mice through inhibiting XOD and ADA activities and the NF-κB and NLRP3 signaling pathways.

4. Experimental

4.1. Chemicals and reagents

ASX was purchased from Jingzhou Natural Astaxanthin Inc. (Hubei, China). PO, HX, carboxymethylcellulose (CMC-Na) and DAB immunohistochemistry color development kit were obtained from Sangon Biotech (Shanghai, China). Allopurinol (ALL) was purchased from Aladdin (Shanghai, China). The kits for the detection of UA, Cr, BUN, CAT, SOD, GSH-Px, and MDA were ordered from the Jiancheng Bioengineering Institute (Nanjing, China). The kits for enzyme-linked immunosorbent assay (ELISA) and bicinchoninic acid (BCA) protein assay were supplied by Solarbio (Beijing, China). Antibody against ASC was produced by Bioss (Beijing, China). Antibodies against Caspase 1, NF-κB p65, NLRP3, and IkBα were obtained from Proteintech Group, Inc. (Princeton, NJ, USA). Antibodies against p-NF-κB p65, p-IkBα, and cleaved-Caspase-1 were provided from by Affinity Biosciences, Inc. (Cincinnati, OH, USA). DAB immunohistochemistry color development kit was supplied by Boster (Wuhan, China). All reagents else used in this study were of analytical grade.

4.2. Animals and treatments

Eight weeks old male ICR mice (26-28 g) were supplied by the Experimental Animal Center of Zhejiang Province (Hangzhou, China). The animal experiments were strictly conducted following the instructions the Animal Ethics Committee of Zhejiang Ocean University (Zhoushan, China) (Laboratory Animal Certificate No. SCXK ZHE 2019-0031). In this study, all mice were kept under controlled environmental conditions of 22±2 °C, 55±5% humidity and normal light/dark (12 h/12 h) cycle.

After 7 days of adaptive feeding, mice were divided into 6 groups (n=8/group): (1) the Control group (Control); (2) the Model group (Model): the mice were treated with PO and HX; (3) the allopurinol group (ALL): mice were treated with PO, HX, and ALL (5 mg/kg); (4) the low ASX dose group (L-ASX): mice were treated with PO, HX, and ASX (25 mg/kg); (5) the medium ASX dose group (M-ASX): mice were treated with PO, HX, and ASX (50 mg/kg); (6) the high ASX dose group (H-ASX): mice were treated with PO, HX, and ASX (100 mg/kg). To induce hyperuricemia, mice were administered intragastrically with 250 mg/kg PO and 250 mg/kg HX prepared in a 0.5% aqueous solution of sodium CMC-Na. One hour after the administration of PO and HX, mice were treated with either ASX or ALL by oral gavage. Control mice were treated with 0.5% CMC-Na accordingly. These treatments were administered orally once daily for 14 days, and all mice were fed pre-weighed amount of food. On day 15, mice were euthanized 1 h after the final administered dose; the blood samples and tissues of the liver and kidney were collected and stored at -80 °C. The kidney index was calculated as follows:

$$\text{kidney index (\%)} = \frac{\text{weight of kidney (mg)}}{\text{body weight (g)}} \times 100\%$$

4.3. Biochemical analysis

The serum was separated from the retroorbital whole blood (3500 ×g, 5 min). Referring to the methods of Zheng et al. (2019), the kidney and liver tissues homogenate supernatant (10% kidney or liver tissues within ice-cold normal saline, g/g) were prepared from the frozen kidney and liver tissues to detected the activities of XOD and ADA in the liver, the content of MDA, the activities of antioxidant enzymes (GSH-Px, SOD, and CAT) and the levels of TNF-α, IL-6, and IL-1β in the kidney. The protein concentration was quantified by the BCA total protein assay kit in liver and kidney homogenate supernatant. The levels of UA, Cr, BUN, TNF-α, IL-6, and IL-1β in serum were measured based on the manufacturer's instructions.

4.4. Histological assessment

The kidney tissues were fixed in neutral 4% formalin for 24 h and then gradually dehydrated with gradient alcohol. The specimen
s were embedded in paraffin, then cut into 4 μm thick pieces using a microtome (Leica RM2135, Leica Instruments GmbH, Wetzlar, Germany). The sections were stained with hematoxylin and eosin (H&E), then the pathological changes of renal tubules, glomeruli, and kidneys were examined under an optical microscope (Biomicroscope CX31, Olympus, Japan) at magnification of (200×) or (400×).

4.5. Immunohistochemistry analyses of kidney

The paraffin-embedded kidney sections with a thickness of 4 μm were deparaffinized in xylene, gradually rehydrated with gradient alcohol and immersed in 3% H_2O_2 for 10 min. The sections were incubated with BSA at 37 °C for 30 min. Subsequently, the sections were reacted with p-NF-κB p65 or NLRP3 antibody at 4 °C overnight. Then the sections were incubated with a secondary antibody for 30 min, developed with DAB and counterstained with hematoxyline. The protein expressions were analyzed by Image J software.

4.6. Western blot analysis

For protein extraction, the liver tissue was ground in liquid nitrogen, and the powder was collected in a 1.5 mL tube containing prepared cell lysate to lyse the cells. After centrifugation, the protein-containing supernatant was collected. The concentration of protein was detected by BCA protein assay kit. For western blot analysis, protein samples (30 μg of total protein) were separated by 12% sodium-dodecylsulphate polyacrylamide gel electrophoresis (SDS-PAGE) and transferred to activated nitrocellulose membranes. After incubation with primary and secondary antibodies, target bands were detected with Enhanced Chemiluminescence (ECL, Solarbio, Beijing, China). The images were acquired using Alpha FluorChem FC3 imaging system (ProteinSimple, San Jose, CA, USA). Image Lab software was used to analyze protein expressions. GAPDH was used as an internal control.

4.7. Statistical analysis

All data are presented as means±SEM. The significance difference among groups was assessed by one-way ANOVA, followed by the Tukey-Kramer test using SPSS 22 software. The difference is considered significant at P values $P < 0.05$.

Acknowledgments: This research was financially supported by the National Natural Science Foundation of China (grant No.21808208), the Zhejiang Provincial Science and Technology Innovation Program (grant No.2021R411030), and the Fundamental Research Funds for Zhejiang Provincial Universities and Research Institutes (grant No.2020J00001).

Conflicts of interest: None declared.

CRediT authorship contribution statement: Jiangchao Zhuang: Validation, Investigation, Writing – original draft. Xie Zhou: Validation, Investigation, Writing – original draft. Ting Liu: Resources, Data curation. Shuai Zhang: Data curation, Software. Falei Yuan: Data curation, Software. Leifang Zhang: Data curation, Software. Zuisu Yang: Resources. Chen Yan: Conceptualization, Project administration, Funding acquisition, Writing – review & editing.

References

Akca G, Eren H, Tumkaya L, Mercantepe T, Horsanali MO, Deveci E, Dil E, Yilmaz A (2018) The protective effect of astaxanthin against cisplatin-induced nephrotoxicity in rats. Biomed Pharmacother 100: 575–582.

Anders HJ, Suarez-Alvarez B, Grigorescu M, Foresto-Neto O, Steiger S, Desai J, Marschner JA, Honarpisheh M, Shi C, Jordan J, Muller L, Burzlaff N, Bauerle T, Mulay SR (2018) The macrophage phenotype and inflammasome component NLRP3 contributes to nephrocalcinosis-related chronic kidney disease independent from IL-1-mediated tissue injury. Kidney Int 93: 656–669.

Cabau G, Crisan TO, Kluck V, Popp RA, Joosten LAB (2020) Urate-induced immune programming: Consequences for gouty arthritis and hyperuricemia. Immunol Rev 294: 92–105.

Chau YT, Chen HY, Lin PH, Hsia SM (2019) Preventive effects of fucoidan and fucoxanthin on hyperuricemic rats induced by potassium oxonate. Mar Drugs 17: 343.

Chen L, Lan Z (2017) Polydatin attenuates potassium oxonate-induced hyperuricemia and kidney inflammation by inhibiting NF-κB/NLRP3 inflammasome activation via the AMPK/SIRT1 pathway. Food Funct 8: 1785–1792.

Chen Y, Li C, Duan S, Yuan X, Liang J, Hou S (2019) Curcumin attenuates potassium oxonate-induced hyperuricemia and kidney inflammation in mice. Biomed Pharmacother 118: 109195.

Chen Z, Li W, Shi L, Jiang L, Li M, Zhang C, Peng H (2020) Kidney-targeted astaxanthin natural antioxidant nanosystem for diabetic nephropathy therapy. Eur J Pharm Biopharm 156: 143–154.

Shih CC, Hwang HR, Chang CI, Su HM, Chen PC, Kuo HM, Li PJ, Wang HD, Tsui KH, Lin YC, Huang SY, Wen ZH (2017) Anti-inflammatory and antinociceptive effects of ethyl acetate fraction of an edible red macroalgae sarcodia ceylanica. Int J Mol Sci 18: 2437.

Choi WJ, Ford ES, Curhan G, Rankin JI, Choi HK (2012) Independent association of serum retinol and beta-carotene levels with hyperuricemia: A national population study. Arthritis Care Res (Hoboken) 64: 389–396.

Cui D, Liu S, Tang M, Lu Y, Zhao M, Mao R, Wang C, Yuan Y, Li L, Chen Y, Cheng J, Lu Y, Liu J (2020) Phloretin ameliorates hyperuricemia-induced chronic renal dysfunction through inhibiting NLRP3 inflammasome and uric acid reabsorption. Phytomedicine 66: 153111.

Dalbeth N, Choi HK, Joosten LAB, Khanna PP, Matsuo H, Perez-Ruiz F, Stamp LK (2019) Gout. Nat Rev Dis Primers 5: 69.

Das P, Panda SK, Agarwal B, Behera S, Ali SM, Pulse ME, Solomkin JS, Opal SM, Bhandari V, Acharya S (2019) Novel chitohexaose analog protects young and aged mice from CLP induced polymicrobial sepsis. Sci Rep 9: 2904.

Domingueti CP, Dusse LM, Carvalho Md, de Sousa LP, Gomes KB, Fernandes AP (2016) Diabetes mellitus: The linkage between oxidative stress, inflammation, hypercoagulability and vascular complications. J Diabetes Complicat 30: 738–745.

Guo S, Guo L, Fang Q, Yu M, Zhang L, You C, Wang X, Liu Y, Han C (2021) Astaxanthin protects against early acute kidney injury in severely burned rats by inactivating the TLR4/MyD88/NF-kappaB axis and upregulating heme oxygenase-1. Sci Rep 11: 6679.

He W, Su G, Sun-Waterhouse D, Waterhouse GIN, Zhao M, Liu Y (2019) In vivo anti-hyperuricemic and xanthine oxidase inhibitory properties of tuna protein hydrolysates and its isolated fractions. Food Chem 272: 453–461.

Hornung V, Bauernfeind F, Halle A, Samstad EO, Kono H, Rock KL, Fitzgerald KA, Latz E (2008) Silica crystals and aluminum salts activate the NALP3 inflammasome through phagosomal destabilization. Nat Immunol 9: 847–856.

Hung SI, Chung WH, Liou LB, Chu CC, Lin M, Huang HP, Lin YL, Lan JL, Yang LC, Hong HS, Chen MJ, Lai PC, Wu MS, Chu CY, Wang KH, Chen CH, Fann CS, Wu JY, Chen YT (2005) HLA-B*5801 allele as a genetic marker for severe cutaneous adverse reactions caused by allopurinol. Proc Natl Acad Sci USA 102: 4134–4139.

Jiang LL, Gong X, Ji MY, Wang CC, Wang JH, Li MH (2020) Bioactive compounds from plant-based functional foods: A promising choice for the prevention and management of hyperuricemia. Foods 9: 937.

Jiang SQ, Zhang ZW, Huang FF, Yang ZS, Yu FM, Tang YP, Ding GF (2020) Protective effect of low molecular weight peptides from *Solenocera crassicornis* head against cyclophosphamide-induced nephrotoxicity in mice via the Keap1/Nrf2 pathway. Antioxidants-Basel 9: 745.

Niu HS, Liu IM, Niu CS, Ku PM, Hsu CT, Cheng JT (2016) Eucommia bark (Du-Zhong) improves diabetic nephropathy without altering blood glucose in type 1-like diabetic rats. Drug Des Devel Ther 10: 971–978.

Kim HR, Shin DY, Chung KH (2017) In vitro inflammatory effects of polyhexamethylene biguanide through NF-κB activation in A549 cells. Toxicol in Vitro 38: 1–7.

Kim IY, Han KD, Kim DH, Eun Y, Cha HS, Koh EM, Lee J, Kim H (2019) Women with metabolic syndrome and general obesity are at a higher risk for significant hyperuricemia compared to men. J Clin Med 8: 837.

Le Y, Zhou X, Zheng J, Yu F, Tang Y, Yang Z, Ding G, Chen Y (2020) Anti-Hyperuricemic effects of astaxanthin by regulating xanthine oxidase, adenosine deaminase and urate transporters in rats. Mar Drugs 18: 610.

Li K, Deng G, Deng Y, Chen S, Wu H, Cheng C, Zhang X, Yu B, Zhang K (2019) High cholesterol inhibits tendon-related gene expressions in tendon-derived stem cells through reactive oxygen species-activated nuclear factor-κB signaling. J Cell Physiol 234: 18017–18028.

Li L, Chen Y, Jiao D, Yang S, Li L, Li P (2020) Protective effect of astaxanthin on ochratoxin A-induced kidney injury to mice by regulating oxidative stress-related NRF2/KEAP1 pathway. Molecules 25: 1386.

Li X, Zou Y, Xing J, Fu YY, Wang KY, Wan PZ, Zhai XY (2020) Pretreatment with roxadustat (FG-4592) attenuates folic acid-induced kidney injury through antiferroptosis via Akt/GSK-3 β /Nrf2 pathway. Oxid Med Cell Longev 2020: 6286984.

Lin KC, Lin HY, Chou P (2000) The interaction between uric acid level and other risk factors on the development of gout among asymptomatic hyperuricemic men in a prospective study. J Rheumatol 27: 1501–1505.

Linker RA, Zhou Y, Fang L, Jiang L, Wen P, Cao H, He W, Dai C, Yang J (2012) Uric acid induces renal inflammation via activating tubular NF-κB signaling pathway. PLoS One 7: e39738.

Liu H, Zhang XM, Wang YL, Liu BC (2014) Prevalence of hyperuricemia among Chinese adults: a national cross-sectional survey using multistage, stratified sampling. J Nephrol 27: 653–658.

Liu S, Yuan Y, Zhou Y, Zhao M, Chen Y, Cheng J, Lu Y, Liu J (2017) Phloretin attenuates hyperuricemia-induced endothelial dysfunction through co-nhibiting inflammation and GLUT9-mediated uric acid uptake. J Cell Mol Med 21: 2553–2562.

Meng X, Mao Z, Li X, Zhong D, Li M, Jia Y, Wei J, Yang B, Zhou H (2017) Baicalein decreases uric acid and prevents hyperuricemic nephropathy in mice. Oncotarget 8: 40305–40317.

Molteni M, Gemma S, Rossetti C (2016) The role of toll-like receptor 4 in infectious and noninfectious inflammation. Mediat Inflamm 2016: 6978936–6978936.

Oh TR, Choi HS, Kim CS, Bae EH, Ma SK, Sung SA, Kim YS, Oh KH, Ahn C, Kim SW (2019) Hyperuricemia has increased the risk of progression of chronic kidney disease: propensity score matching analysis from the KNOW-CKD study. Sci Rep 9: 6681.

Pelegrin P, Surprenant A (2009) Dynamics of macrophage polarization reveal new mechanism to inhibit IL-1β release through pyrophosphates. EMBO J 28: 2114–2127.

Qian X , Wang X , Luo J , Liu Y , Pang J , Zhang H , Xu Z , Xie J , Jiang X , Ling W (2019) Hypouricemic and nephroprotective roles of anthocyanins in hyperuricemic mice. Food Funct 10: 867–878.

Sutterwala FS, Haasken S, Cassel SL (2014) Mechanism of NLRP3 inflammasome activation. Ann NY Acad Sci 1319: 82–95.

Wei Z, Xi J, Gao S, You X, Li N, Cao Y, Wang L, Luan Y, Dong X (2018) Metabolomics coupled with pathway analysis characterizes metabolic changes in response to BDE-3 induced reproductive toxicity in mice. Sci Rep 8: 5423.

Huang TH, Chen YT, Sung PH, Chiang HJ, Chen YL, Chai HT, Chung SY, Tsai TH, Yang CC, Chen CH, Chen YL, Chang HW, Sun CK, Yip HK (2016) Peripheral blood-derived endothelial progenitor cell therapy prevented deterioration of chronic kidney disease in rats. Am J Transl Res 7: 804–824.

Xiao N, Qu J, He S, Huang P, Qiao Y, Li G, Pan T, Sui H, Zhang L (2020) Exploring the therapeutic composition and mechanism of Jiang-Suan-Chu-Bi recipe on gouty arthritis using an integrated approach based on chemical profile, network pharmacology and experimental support using molecular cell biology. Front Pharmacol 10: 1626.

Yip K, Cohen RE, Pillinger MH (2020) Asymptomatic hyperuricemia: is it really asymptomatic? Curr Opin Rheumatol 32: 71–79.

Yuan Z, Liling D, Chunmei W, Lianji Z, Geng Z (2018) Konjac glucomannan improves hyperuricemia through regulating xanthine oxidase, adenosine deaminase and urate transporters in rats. J Funct Foods 48: 566–575.

Zhang D, Liu H, Luo P, Li Y (2018) Production inhibition and excretion promotion of urate by fucoidan from laminaria japonica in adenine-induced hyperuricemic mice. Mar Drugs. 16: 472.

Zhang ZC, Zhou Q, Yang Y, Wang Y, Zhang JL (2019) Highly acylated anthocyanins from purple Sweet Potato (Ipomoea batatas L.) alleviate hyperuricemia and kidney inflammation in hyperuricemic mice: Possible attenuation effects on zllopurinol. J Agric Food Chem 67: 6202–6211.

Zhao XJ, Yang YZ, Zheng YJ, Wang SC, Gu HM, Pan Y, Wang SJ, Xu HJ, Kong LD (2017) Magnesium isoglycyrrhizinate blocks fructose-induced hepatic NF-κB/NLRP3 inflammasome activation and lipid metabolism disorder. Eur J Pharmacol 809: 141–150.

Zheng J, Tian X, Zhang W, Zheng P, Huang F, Ding G, Yang Z (2019) Protective effects of fucoxanthin against alcoholic liver injury by activation of Nrf2-mediated antioxidant defense and inhibition of TLR4-mediated inflammation. Mar Drugs 17: 552.

Zhou Y, Fang L, Jiang L, Wen P, Cao H, He W, Dai C, Yang J (2012) Uric acid induces renal inflammation via activating tubular NF-κB signaling pathway. PLoS One 7: e39738.